Nanomedicine

International Edition: DOI: 10.1002/anie.201503863
German Edition: DOI: 10.1002/ange.201503863

Hydrophobic Cysteine Poly(disulfide)-based Redox-Hypersensitive Nanoparticle Platform for Cancer Theranostics**

*Jun Wu, Lili Zhao, Xiaoding Xu, Nicolas Bertrand, Won Il Choi, Basit Yameen, Jinjun Shi, Vishva Shah, Matthew Mulvale, James L. MacLean, and Omid C. Farokhzad**

Abstract: *Selective tumor targeting and drug delivery are critical for cancer treatment. Stimulus-sensitive nanoparticle (NP) systems have been designed to specifically respond to significant abnormalities in the tumor microenvironment, which could dramatically improve therapeutic performance in terms of enhanced efficiency, targetability, and reduced side-effects. We report the development of a novel* L*-cysteine-based poly (disulfide amide) (Cys-PDSA) family for fabricating redox-triggered NPs, with high hydrophobic drug loading capacity (up to 25 wt % docetaxel) and tunable properties. The polymers are synthesized through one-step rapid polycondensation of two nontoxic building blocks:* L*-cystine ester and versatile fatty diacids, which make the polymer redox responsive and give it a tunable polymer structure, respectively. Alterations to the diacid structure could rationally tune the physicochemical properties of the polymers and the corresponding NPs, leading to the control of NP size, hydrophobicity, degradation rate, redox response, and secondary self-assembly after NP reductive dissociation. In vitro and in vivo results demonstrate these NPs' excellent biocompatibility, high selectivity of redox-triggered drug release, and significant anticancer performance. This system provides a promising strategy for advanced anticancer theranostic applications.*

Since the 1970s, nanoparticle (NP)-based systems could enhance efficacy, decrease toxicity, and improve the circulation and biodistribution of therapeutic payloads, whether they are small molecules, proteins, or nucleic acids.[1–8] Owing to their scale and distinct physicochemical properties as well as the specific pathophysiological characteristics of tumors, NPs offer the potential to significantly improve cancer diagnosis and therapy.[9,10] Additionally, NPs that are selectively responsive to environmental stimuli offer spatiotemporal control of the delivery of anticancer therapeutics.[11] As previously reported, NPs could increase the local accumulation inside the tumor, improve homogeneous spatial distribution, and enhance intracellular localization of drugs.[10] In that regard, multiple NP systems have been designed to respond to distinct exogenous and endogenous stimuli like light,[12] magnetic fields,[13,14] ultrasound,[15] enzymes,[16] pH,[17,18] temperature,[19] and altered redox potential.[20,21] Hypoxia has been recognized as one of the unique hallmarks of cancer and significantly alters local redox microenvironments within tumor tissue. The intracellular levels of glutathione are 100–1000 fold higher in cancer cells than in normal tissue.[22] This redox-sensitive approach is particularly promising to enhance the exposure of cancer cells to therapeutic molecules. Additionally, because hypoxic characteristics play a critical role in tumor progression as tumor invasion, metastasis, and therapeutic resistance,[23] exploiting them to selectively improve the release of payloads might provide added therapeutic benefits.

Over the years, various disulfide-based NP systems have been proposed for gene delivery and cancer therapy.[24–26] They were designed to remain stable in the bloodstream and protect their therapeutic payloads from extracellular degradation, while allowing rapid drug release upon reduction of the disulfide bonds after cell uptake.[26] However, the applications of disulfide systems are subject to several limitations, such as complicated synthesis strategy, lack of tunable properties/functionalities, and lack of biocompatibility.[26] Despite being the most natural sulfur-containing materials in body, L-cysteine and its derivatives have rarely been systematically utilized as building blocks to develop linear disulfide polymers, especially hydrophobic polymers for drug delivery.

[*] Dr. J. Wu,[+] Dr. L. Zhao,[+] Dr. X. Xu,[+] Dr. W. I. Choi, Dr. B. Yameen, Prof. J. Shi, V. Shah, M. Mulvale, J. L. MacLean, Prof. O. C. Farokhzad
Laboratory of Nanomedicine and Biomaterials, Department of Anesthesiology, Brigham and Women's Hospital
Harvard Medical School
Boston, MA 02115 (USA)
E-mail: ofarokhzad@zeus.bwh.harvard.edu
Dr. L. Zhao[+]
Department of Endoscopy, the First Affiliated Hospital of Nanjing Medical University, Jiangsu Province Hospital
Nanjing, Jiangsu, 210029 (P.R. China)
Dr. N. Bertrand
David H. Koch Institute for Integrative Cancer Research
Massachusetts Institute of Technology
Cambridge, MA 02139 (USA)
Prof. O. C. Farokhzad
King Abdulaziz University, Jeddah (Saudi Arabia)
[+] These authors contributed equally to this work.

[**] This research was supported by the National Institutes of Health under grant number CA151884, EB015419-01, the Movember-Prostate Cancer Foundation Challenge Award, the National Research Foundation of Korea K1A1A2048701, and the David Koch-Prostate Cancer Foundation Program in Cancer Nanotherapeutics. O.C.F. has financial interest in BIND Therapeutics, Selecta Biosciences, and Blend Therapeutics, biopharmaceutical companies that are developing therapeutic nanoparticles. N.B. acknowledges a postdoc fellowship from the Canadian Institute of Health Research (CIHR). J.S. acknowledges support from NCI R00A160350 and PCF Young Investigator Award.

Supporting information for this article is available on the WWW under http://dx.doi.org/10.1002/anie.201503863.

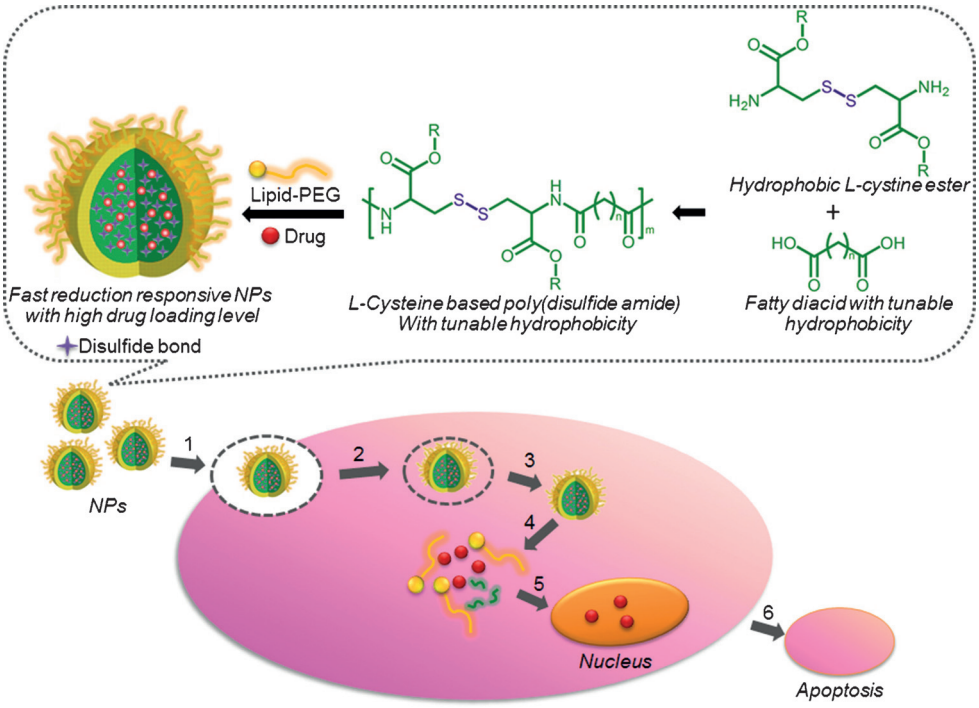

Scheme 1. Illustration of L-cysteine-based poly(disulfide amide) and intracellular delivery of docetaxol-loaded redox-responsive Cys-PDSA NPs.

Here we report the development of a novel biodegradable and biocompatible L-cysteine-based poly(disulfide amide) (Cys-PDSA) that is prepared simply, rapidly, and under mild reaction conditions (Scheme 1 and Figure S1a). A typical Cys-PDSA structure includes two nontoxic repeating units: one disulfide part (L-cystine ester) and one diacid part (aliphatic dicarboxylic acid). The L-cystine ester provides primitive redox-responsive characteristics based on its disulfide bond. With introduction of varied diacid segments, polymer properties can be finely tuned for rationally designing the NPs' hydrophobicity and redox response. To develop a versatile, safe, and easy-to-synthesize redox-responsive polymer platform for preparing selectively targeting polymeric NPs, the direct polycondensation route of cystine esters and diacid monomers was chosen because it is mild and efficient. To warrant optimal drug loading capacity and maximal adaptability, it should be able to fine-tune the hydrophobicity and degradability of the polymer by altering the diacid repeating unit. Esters of cystine offer simple synthesis routes using derivatives of a natural amino acid while ensuring sufficient hydrophobicity to warrant solubility in organic solvents. This latter characteristic is important for polymer synthesis and NP preparation and also safeguards increased interactions with hydrophobic payloads. As a model cystine ester, L-cystine dimethyl ester was chosen, because it is commercially available, reasonably stable, and simple in structure. Similarly, different fatty diacids of variable lengths are also available. Together, these combinations of monomers allow tuning of the physicochemical properties of the backbone on two fronts: hydrophobicity and the density of the disulfide bonds. A library of polymers with a backbone consisting of alternating biodegradable amide and disulfide bonds can therefore be prepared using different combinations.

In this report, Cys-PDSA polymers were prepared within 5–10 min by one-step polycondensation of $(H\text{-Cys-OMe})_2\cdot 2HCl$ and dichlorides or bis-nitrophenol esters of different fatty diacids (Figure S1a). The synthesis protocol of Cys-PDSAs was optimized and the detailed composites and final PDSA structures are summarized in Table S1. These prepared PDSAs are named as Cys-xE, with x representing the number of methylene groups in the diacid repeating unit and E indicating the methyl ester of carboxylic acid on the side chain (see the Supporting Information, SI). The molecular weight and terminal functionality were controlled by varying the ratio of the two monomers and the optimal synthesis was obtained after 5–10 min reaction time at 25.0 °C in DMSO (or chloroform) with triethylamine as catalyst. Short reaction times were preferred to prevent unwanted side reactions (i.e., production of dark-colored by-products, etc.). Under those conditions, the polycondensation provided reasonable yields (>70%) with typical M_n ranging from 10.0 kg mol^{-1} to 20.0 kg mol^{-1} and polydispersity indexes of 1.20–1.50. Although the chain length of the fatty diacid had a distinctive influence on the physicochemical properties of the material, it did not appear to significantly affect the molecular weight or polydispersity of polymers. Differential scanning calorimetry (DSC) on the polymers showed that only Cys-10E exhibited a sharp melting point (T_m) around 60 °C, suggesting a semicrystalline structure, whereas the other polymers ($x = 2$–8) showed amorphous behavior (SI). The glass transition temperature (T_g) for these polymers ranged from 20–44 °C (Table S1). For polymers with diacid monomers containing two, four, and six methylene units, the T_g decreased inversely to the length of the fatty diacid chain, whereas the T_g returned to 27 °C for the sebacoyl chloride monomer (Cys-8E) (Figures S2–S6). The chemical structures of the polymers were confirmed by ^{1}H NMR spectroscopy (Figures 1 A and S7–S10).

For the preparation of NPs with hydrophobic cores and high drug loading, the solubility of the polymer in different environments is important. We deemed a polymer to be soluble at room temperature if dissolution of $\geq$1.0 mg mL^{-1} was possible. The prepared Cys-PDSAs were found to be insoluble in aqueous solutions and organic solvents with polarity index below 2.8 (benzene, toluene, and ethyl ether).

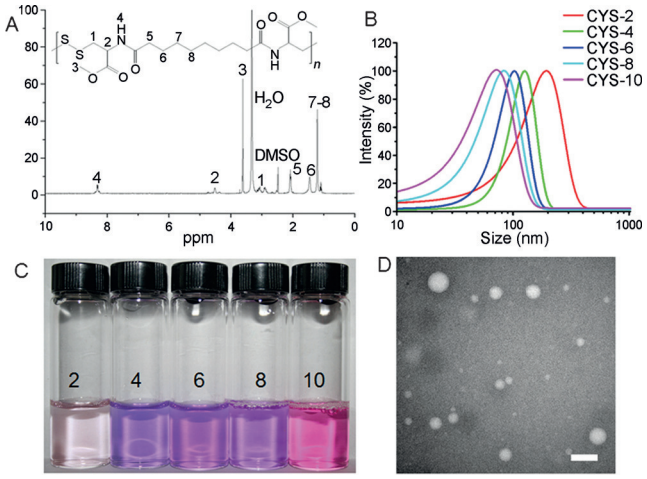

Figure 1. A) ^{1}H NMR spectrum of Cys-8E. B) Particle size of Cys-*x*E NPs (*x* from 2 to 10). C) Cys-*x*E NP solutions loaded with 1 wt% Nile red to demonstrate differences in hydrophobicity (from left to right: *x* = 2,4,6,8,10). D) TEM images of Cys-8E NPs (scale bar = 100 nm).

In contrast, they were soluble in more polar organic solvents (DMSO, DMF, THF, chloroform, and dichloromethane). This extended range of solubility in a variety of water-miscible and water-immiscible organic solvents is ideal to allow the preparation of NPs using various methods, but also to simplify the fabrication of multiple types of matrices from these polymers. Owing to their broad solubility in various solvents, NPs containing Cys-PDSAs can be prepared by nanoprecipitation as well as single or double emulsions. Among those fabrication methods, nanoprecipitation from DMSO offered the most simplicity and reproducibility and was chosen for further study. Under a standardized protocol (SI), the different polymers produced NPs of different hydrodynamic sizes (Figure 1 B). Polymers with longer fatty diacid chains provided smaller NPs with possibly more dehydrated and compact cores due to the increased hydrophobicity. TEM imaging confirmed the size and spherical morphology of the NPs (Figure 1 D). Different stabilizers were screened to improve the colloidal stability of the Cys-PDSA NPs, including PVA, Tween, Pluronic, PEG, MYRJ, Lipid, and PEGylated-lipids (SI). NPs stabilized with DPSE-mPEG with PEG chains of 3000 Da showed better colloidal stability after incubation in PBS or 10% FBS media (Figure S11). The stabilizer concentration was optimized between 15–30 wt% of the NPs. It is expected that hybrid NPs consisting of a Cys-PDSA core surrounded by a monolayer of lipids will self-assemble upon introduction of the DMSO polymer solution in water. The zeta potential of the NPs finally ranged from −10 to −30 mV. Encapsulation of 1 wt% of Nile red, an environment-dependent fluorescent probe, was used to ascertain the hydrophobicity of the NPs. Figure 1 C shows that the color intensity of the dye increases with the length of fatty acid units, suggesting the increasing hydrophobicity in the core. NPs prepared by poly(disulfide)s with shorter diacid chains show weaker color intensity, indicating lower hydrophobicity.

Disulfide bonds are prone to cleavage in a reductive environment through the dithiol–disulfide exchange reaction. Due to the high density and even distribution of disulfide bonds along the Cys-PDSA polymer chain, the Cys-PDSA NPs were designed for disassembly/degradation under reducing environments. The fluorescence of Nile red was used as an indicator of polymer degradation and NP disassembly. Although polymer Cys-2E could not be evaluated because of poor dye encapsulation, the other Cys-PDSA polymers (*x* = 4, 6, 8, and 10) were tested. As shown in Figure 2 a,

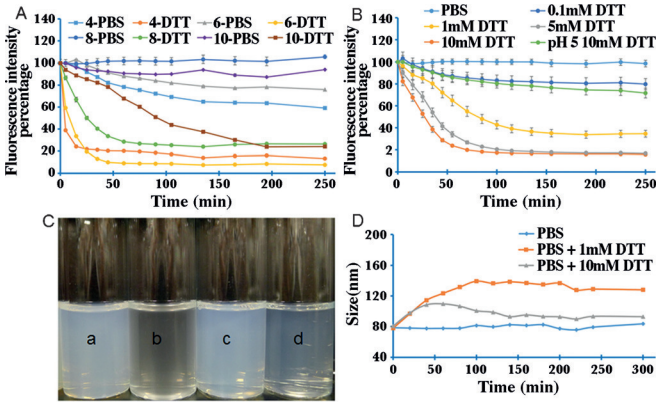

Figure 2. A) Fluorescence intensity changes for different Cys-PDSA NPs under PBS and 10 mM DTT. B) Fluorescence intensity change for Cys-8E NPs under different DTT conditions. C) Appearance of Cys-8E NP solutions after 2 h reduction (from left to right: blank (Cys-8E NP in distilled water), Cys-8E NP solution with 10 mM DTT, Cys-8E NP PBS solution with 20 wt% DSPE-mPEG3000, Cys-8E NP PBS solution with 10 mM DTT and 20 wt% DSPE-mPEG3000. D) Particle size change for Cys-8E NPs with different DTT concentrations.

whereas NPs prepared with Cys-4E and Cys-6E appeared to lose 20–40% of their initial fluorescence over 4 h of incubation in 37 °C PBS, the fluorescence intensity of NPs prepared with Cys-8E and Cys-10E did not change. This suggests that polymers made out of monomers with eight and ten methylene groups exhibit improved Nile red retention and slower release rates of their cargo, possibly due to increased hydrophobic interactions with the dye and denser packing of the polymer core. 10 mM DTT PBS solution is widely used to mimic the intracellular redox-environment of common tumors.[25] Under such conditions,[25] the fluorescence rapidly decreased for all NPs. Interestingly, the susceptibility of the NPs to the reducing agent also appears to be influenced by the nature of the polymers, with higher *x* values exhibiting slower DTT-triggered release of Nile red. NPs prepared with Cys-4E completely disassembled after 20 min, whereas Cys-6E and Cys-8E NPs needed between 30 and 60 min. For NPs prepared with Cys-10E, the rate of disassembly was relatively low, and the fluorescence intensity kept decreasing for about 3 h. Once again, the degradation of the NPs is consistent with the hydrophobicity of the polymer and the chain length of the diacid monomers. 10 mM glutathione (GSH) PBS solution shows similar effects on the Nile red release profile (SI, Figure S12). GPC results also confirmed that the molecular weight of Cys-8E shows significant reduction after GSH treatment (Figure S13).

Based on redox-responsive sensitivity, hydrophobicity, and NP characteristics, the susceptibility of Cys-8E NPs to different concentrations of reducing agents was studied. Figure 2b demonstrates that the NP disassembling rate was accelerated with increasing concentrations of DTT. Although the Nile red release rates were similar upon incubation with 5.0 and 10.0 mM DTT, no noticeable disassembly was observed for 0.1 mM DTT over 4 h. These conditions correspond to a redox potential similar to those observed in extracellular fluids.[25] Interestingly, the pH of the solution appears also to affect the NP susceptibility to the reducing agent. At pH 5, 10 mM DTT was not able to trigger disassembly, suggesting that redox-mediated release of the payloads might selectively occur in the cytosol instead of the endosome/lysosome, potentially conferring intracellular targeting properties to the NPs. Furthermore, Figure 2C showed the effect of NP stabilizer on 10 mM DTT disassembly. After 2 h, unlike Cys-8E NP in distilled water, Cys-8E NP solution with 10 mM DTT turned from a milky solution to clear, indicating that the majority of the NPs are degraded. Compared with the combination of Cys-8E NP PBS solution and 20 wt% DSPE-mPEG3000, the mixture of Cys-8E NP PBS solution with 10 mM DTT and 20 wt% DSPE-mPEG3000 showed slower degradation (from milky to less milky).

The impact of exposure to the reducing agent on the hydrodynamic diameter of the NPs was investigated by DLS. Figure 2d shows that the particle size increased slightly after the addition of DTT (1 mM and 10 mM). For longer periods, the size of the NP remained stable and the count rate decreased with time. To characterize the particles' morphology during the disassembling procedure, TEM was utilized to monitor the structure of the degraded products. TEM imaging (Figure S14) showed that two types of structures were formed: degraded, irregularly shaped NP debris from a few to tens of nm, or spherical shapes ranging from hundreds to thousands of nm. This spherical structure was observed only for $x = 8$ and 10. One possible reason could be the specific hydrophobic structure of the polymer Cys-8E and Cys-10E, causing some secondary self-assembly of the degraded polymer segments during or after the NP disruption. As shown in Figure 2d, partial degradation under 1 mM DTT resulted in a stronger secondary assembly and large changes in size. Therefore, DTT induced NP changes through degradation and reassembly. This phenomenon inspired that rapid degradation could trigger pulse-high dosage treatment, while partial reassembly may locally lead to aggregated particles and drug sustained-release for long-term therapy. Although these results are very preliminary, this redox degradation and secondary self-assembly phenomenon could be an interesting topic for further investigation. Based on TEM images and the above discussions, we could draw two conclusions about the redox degradation of the Cys-PDSA NPs: 1) all NPs are almost completely degraded within a few hours, and 2) the secondary self-assembly may happen for NPs with high hydrophobicity.

To ascertain the biocompatibility of the polymer, the cytotoxicity of Cys-PDSA NPs coated with 20 wt% DSPE-mPEG3000 was studied on HeLa cells after 48 h exposure. None of the NPs appeared to cause any obvious cellular toxicity (Figure S17). During in vivo evaluation in mice, weight change (Figure S19) and histopathology of main organs (Figure S22) also confirmed the good biocompatibility of Cys-8E NPs. The intracellular redox sensitivity of the NPs was studied using a co-encapsulated Förster resonance energy transfer (FRET) pair consisting of hydrophobic coumarin 6 (400Ex/510Em) and Nile red (520Ex/590Em). In this experiment, upon excitation of the donor dye (coumarin 6, excited at 400 nm), the emitted energy is transferred to the acceptor dye (Nile red) due to its close proximity (< 10 nm), and it is able to fluoresce (at 590 nm). Upon disassembly of the NPs, the FRET pair is separated and the normal fluorescence of the coumarin dye is restored, whereas the Nile red stops fluorescing. The ratio of Nile red to coumarin 6 has been optimized at 10:1. As shown in Figure 3, after 0.5 h treatment,

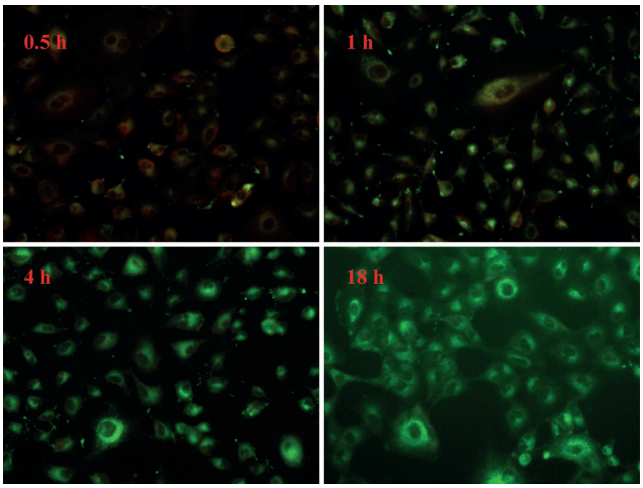

Figure 3. FRET effect for Cys-8E/DSPE-mPEG3000 hybrid NPs with 0.1 wt% coumarin 6 and 1 wt% Nile red. A549 cells were used. Cells with some red or orange color means the NPs are not completely dissociated; the green color indicates that NPs are completely dissociated.

obvious NP uptake and FRET effect were observed inside A549 cells. After 1 h, the red fluorescence resulting from the FRET decreases, whereas the green fluorescence of coumarin 6 increases. After 4 h, the cells show a dominant green color, and the red color is difficult to detect. After 18 h, there was no visible red fluorescence inside the cells. All these images indicate that these hydrophobic NPs exhibit a relatively fast cellular uptake (within a few hours) and efficient redox-sensitivity inside tumor cells. When A549 cells were pretreated with 50 μM *N*-ethylmaleimide (NEM) for 1 h,[27] the FRET effect persisted after 4 h treatment with NPs (Figure S15), indicating that GSH-triggered reduction was significantly inhibited. These intracellular degradation performances were consistent with previously observed in vitro disassembly behavior of Nile-red loaded Cys-8E NPs.

Although docetaxel (Dtxl) has undeniable efficacy to treat various types of cancer, its very low solubility in water requires the use of toxic solvents in its formulations. This results in drugs that have greater toxicity and poor tolerance.

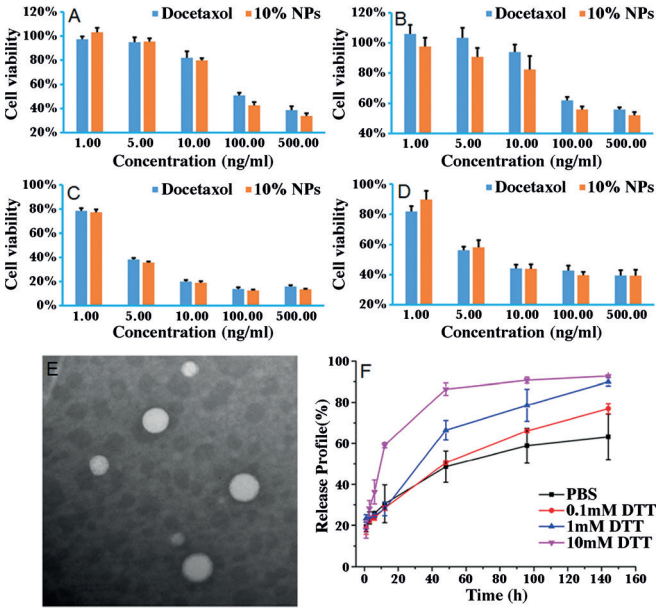

Figure 4. A–D) In vitro anticancer evaluation for DSPE-PEG-coated Cys-8E NPs with 10 wt% Dtxl encapsulated. A) and C) HeLa cells were treated with Dtxl-loaded NPs for 4 h and 48 h, respectively. B) and D) DU145 cells were treated with Dtxl-loaded NPs for 4 h and 48 h, respectively. Cells treated with free Dtxl were used as controls. E) TEM images of Cys-8E NPs loaded with 20 wt% Dtxl (scale bar = 200 nm). F) Cumulative release of Dtxl from Cys-8E NPs.

Dtxl therefore offers a broadly used model of hydrophobic payload for the preclinical development of drug delivery platforms. Owing to its high hydrophobicity, stability, and selective redox-sensitivity, Cys-8E was selected for the preparation of Dtxl-loaded NPs. Figure 4E is the TEM image of 20 wt% Dtxl-loaded Cys-8E NPs. The loading of a higher amount of drug did not significantly alter NP morphology, but may slightly increase NP size. After optimizing, the maximum Dtxl loading efficiency of Cys-8E NPs could reach 25 wt% of NPs. The Dtxl concentrations of the Cys-PDSA NPs were quantified by HPLC.

Figure 4F shows the results of the in vitro release experiments conducted with Dtxl-loaded Cys-8E NPs. This panel shows that in PBS, the NPs release less than 60% of their drug content over six days. In contrast, upon addition of 1 or 10 mM DTT, the same quantity was released within 48 and 12 h, respectively. Compared with the PBS group, the 1 mM DTT and 10 mM groups showed significantly different Dtxl release performance, confirming the redox-promoted discharge of payload. HeLa, MCF-7, A549, and DU145 cells were used for evaluating the in vitro anticancer performance of Cys-8E NPs with 10 wt% Dtxl. Figure 4A–D shows the cell viability of HeLa and DU145 cells under different treatment conditions. Overall, drug-loaded NPs had anticancer effects similar to free Dtxl without significant differences, though the therapeutic efficacy varied among cell lines. With extension of the treatment period from 4 h to 48 h, both free drug and NPs showed dramatic improvement in inhibition of cell growth. Similar to the cell-uptake results, when HeLa cells were pretreated with 50 μM NEM for 1 h, Glutathione (GSH) depletion inhibited intracellular redox-sensitivity, which further reduced the anticancer performance of Dtxl-loaded Cys-8E NPs (Figure S18). These in vitro performances confirm that Dtxl-loaded NPs could be an interesting platform for anticancer treatment and warrant further investigation in vivo.

The antitumor efficacy of 10 wt% Dtxl-loaded Cys-8E NPs was evaluated in an A549 xenograft mouse model. Prior to the experiment, the maximum tolerance dosage (MTD) of free Dtxl was established in normal mice at 5 mg kg^{-1}. Furthermore, NPs biodistribution and pharmacokinetics (PK) are presented in Figures S20 and S21, respectively. The PK results indicate that docetaxel-loaded Cys-8E NPs and poly(lactic-*co*-glycolic acid) (PLGA) NPs have similar $t_{1/2}$ (around 5.38 h), much better than free Dtxl (around 1.18 h).[28] Although some NPs had been quickly captured inside liver and spleen after administration, the fluorescence intensity of tumor kept increasing due to the enhanced permeation and retention (EPR) effect, indicating improved drug accumulation for cell inhibition. Then the investigational treatments were designed as follows: Group A: PBS; Group B: free Dtxl 5 mg kg^{-1} (Taxotere); Group C: PLGA NPs equivalent to 5 mg kg^{-1} of Dtxl; Group D: Cys-8E NPs equivalent to 5 mg kg^{-1} of Dtxl; Group E: Cys-8E NPs equivalent to 10 mg kg^{-1} of Dtxl. All treatments were injected twice through the lateral tail vein on day 9 and 23 after tumor inoculation. As shown in Figure 5, the PBS control group exhibited rapid tumor growth, whereas free Dtxl and Dtxl-loaded PLGA NPs showed only limited tumor inhibition. In comparison, 5 mg kg^{-1} of Dtxl loaded in NPs suppressed tumor growth for longer. For comparison purposes, the volume of tumors in mice injected with 5 mg kg^{-1} of Dtxl-loaded Cys-8E NPs took 35 days to reach that volume at 28 days in mice treated with 5 mg kg^{-1} of Dtxl. The encapsulation of Dtxl in Cys-8E NPs allowed increasing the dose above the 5 mg kg^{-1} MTD without significant weight loss in mice (Figure S19). The more aggressive treatment (10 mg kg^{-1}) significantly improved tumor inhibition, with tumors not reaching the 300 mm^3 volume before day 48. Although tumor growth was observed in all groups, possibly because the study was designed with only two therapeutic

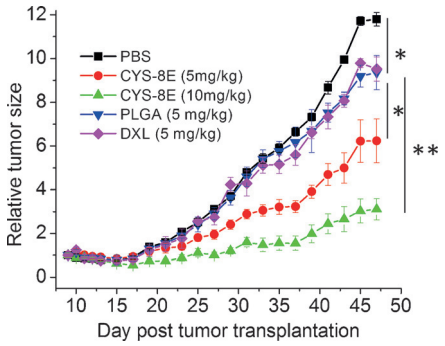

Figure 5. Antitumor activity of Dtxl-loaded Cys-8E NPs. Mice were treated on day 9 and 23 after tumor inoculation. The Dtxl dosage was 5 mg kg^{-1} for each injection. Tumor volume is represented as the mean ± SEM ($n = 5$). Statistical differences among treated groups were determined by one-way ANOVA assay (*$P < 0.05$)

doses, Cys-8E greatly reduced the size of tumors, confirming the potential of redox-responsive polymeric NPs.

In summary, we have developed a new family of biocompatible, biodegradable, fast redox-responsive, and hydrophobic L-cysteine-based poly(disulfide amide)s. These polymers were used to synthesize NPs with great potential for anticancer applications. Using fatty diacid monomers with different numbers of methylene groups, the polymers could be tailored to exhibit distinct properties and kinetics of degradation. Whereas controlling hydrophobicity could be exploited to optimize the encapsulation of therapeutic cargos, the rapid degradation occurring in reducing environments could selectively increase intracellular drug release. Conceivably, tuning of these properties could culminate in more efficient NP systems with improved spatiotemporal delivery of therapeutic payloads.

Keywords: cysteine · disulfide · hydrophobic · polymeric nanoparticle · redox response

How to cite: *Angew. Chem. Int. Ed.* **2015**, *54*, 9218–9223
Angew. Chem. **2015**, *127*, 9350–9355

[1] E. M. Pridgen, F. Alexis, T. T. Kuo, E. Levy-Nissenbaum, R. Karnik, R. S. Blumberg, R. Langer, O. C. Farokhzad, *Sci. Transl. Med.* **2013**, *5*, 213ra167.
[2] D. Peer, J. M. Karp, S. Hong, O. C. FaroKhzad, R. Margalit, R. Langer, *Nat. Nanotechnol.* **2007**, *2*, 751.
[3] O. C. Farokhzad, R. Langer, *Adv. Drug Delivery Rev.* **2006**, *58*, 1456.
[4] J. Wu, N. Kamaly, J. Shi, L. Zhao, Z. Xiao, G. Hollett, R. John, S. Ray, X. Xu, X. Zhang, P. W. Kantoff, O. C. Farokhzad, *Angew. Chem. Int. Ed.* **2014**, *53*, 8975; *Angew. Chem.* **2014**, *126*, 9121.
[5] J. Wu, C.-C. Chu, *J. Mater. Chem. B* **2013**, *1*, 353.
[6] I.-H. Lee, H.-K. Kwon, S. An, D. Kim, S. Kim, M. K. Yu, J.-H. Lee, T.-S. Lee, S.-H. Im, S. Jon, *Angew. Chem. Int. Ed.* **2012**, *51*, 8800; *Angew. Chem.* **2012**, *124*, 8930.
[7] R. Mo, T. Jiang, R. DiSanto, W. Tai, Z. Gu, *Nat. Commun.* **2014**, *5*, 3364.
[8] A. K. Salem, P. C. Searson, K. W. Leong, *Nat. Mater.* **2003**, *2*, 668.
[9] Y. Matsumura, H. Maeda, *Cancer Res.* **1986**, *46*, 6387.
[10] N. Bertrand, J. Wu, X. Xu, N. Kamaly, O. C. Farokhzad, *Adv. Drug Delivery Rev.* **2014**, *66*, 2.
[11] M. Motornov, Y. Roiter, I. Tokarev, S. Minko, *Prog. Polym. Sci.* **2010**, *35*, 174.
[12] J. Liu, Y. Lu, *J. Am. Chem. Soc.* **2005**, *127*, 12677.
[13] J. Zhu, Y. Lu, Y. Li, J. Jiang, L. Cheng, Z. Liu, L. Guo, Y. Pan, H. Gu, *Nanoscale* **2014**, *6*, 199.
[14] S. Giri, B. G. Trewyn, M. P. Stellmaker, V. S. Y. Lin, *Angew. Chem. Int. Ed.* **2005**, *44*, 5038; *Angew. Chem.* **2005**, *117*, 5166.
[15] Y. Uesugi, H. Kawata, J.-i. Jo, Y. Saito, Y. Tabata, *J. Controlled Release* **2010**, *147*, 269.
[16] R. de La Rica, D. Aili, M. M. Stevens, *Adv. Drug Delivery Rev.* **2012**, *64*, 967.
[17] W. Gao, J. M. Chan, O. C. Farokhzad, *Mol. Pharm.* **2010**, *7*, 1913.
[18] N. Bertrand, P. Simard, J.-C. Leroux in *Liposomes*, *Vol. 1* (Ed.: V. Weissig), Humana, Totowa, NJ, **2009**, p. 545.
[19] Z. Xiao, C. Ji, J. Shi, E. M. Pridgen, J. Frieder, J. Wu, O. C. Farokhzad, *Angew. Chem. Int. Ed.* **2012**, *51*, 11853; *Angew. Chem.* **2012**, *124*, 12023.
[20] W. Gao, R. Langer, O. C. Farokhzad, *Angew. Chem. Int. Ed.* **2010**, *49*, 6567; *Angew. Chem.* **2010**, *122*, 6717.
[21] S. Mura, J. Nicolas, P. Couvreur, *Nat. Mater.* **2013**, *12*, 991.
[22] F. Q. Schafer, G. R. Buettner, *Free Radical Biol. Med.* **2001**, *30*, 1191.
[23] J. M. Brown, W. R. Wilson, *Nat. Rev. Cancer* **2004**, *4*, 437.
[24] S. Bauhuber, C. Hozsa, M. Breunig, A. Göpferich, *Adv. Mater.* **2009**, *21*, 3286.
[25] M. Zhao, A. Biswas, B. Hu, K.-I. Joo, P. Wang, Z. Gu, Y. Tang, *Biomaterials* **2011**, *32*, 5223.
[26] E.-K. Bang, M. Lista, G. Sforazzini, N. Sakai, S. Matile, *Chem. Sci.* **2012**, *3*, 1752.
[27] S. Bhuniya, S. Maiti, E.-J. Kim, H. Lee, J. L. Sessler, K. S. Hong, J. S. Kim, *Angew. Chem. Int. Ed.* **2014**, *53*, 4469; *Angew. Chem.* **2014**, *126*, 4558.
[28] E. L. Bradshaw-Pierce, S. G. Eckhardt, D. L. Gustafson, *Clin. Cancer Res.* **2007**, *13*, 2768.

Received: April 27, 2015
Revised: May 20, 2015
Published online: June 26, 2015

